185261

$p. \ 23$

N94-12285

A local dynamic model for large eddy simulation

By S. Ghosal, T. S. Lund AND P. Moin

1. Motivation and objectives

The dynamic model (Germano *et al.* 1991) is a method for computing the coefficient C in Smagorinsky's (1963) model for the subgrid-scale stress tensor as a function of position from the information already contained in the resolved velocity field rather than treating it as an adjustable parameter. There are two advantages to this. Firstly, it gives a systematic procedure for computing a flow about which we have no prior experience and, therefore, cannot properly adjust the parameter C. Secondly, in an inhomogeneous flow, the optimum choice of C may be different at different points in the flow, and one does not expect the entire flow to be represented by a single constant. The same consideration applies to flows undergoing a transition to turbulence or, more generally, to flows whose statistical properties are changing with time. In the traditional approach, one needs to introduce further *ad hoc* assumptions, such as wall damping functions or a prescription to reset the value of C from zero to a finite number as the flow undergoes a transition to turbulence. In contrast, inhomogeneous and statistically unsteady flows can be handled very naturally in the context of the dynamic model since C is now a function of position and time. Though the dynamic model lacked the full generality necessary to handle general turbulent flows with no homogeneous directions, the method had some important successes.

The basic formalism behind the method is summarized below following Germano *et al.* (1991). The equations of LES can be thought of as a filtered form of the Navier-Stokes equations where the filtering serves to remove fluctuations on length-scales smaller than the computational grid. The effect of the unresolved eddies on the large eddies is then manifested through the Reynolds stress term $\tau_{ij} = \overline{u_i u_j} - \overline{u}_i \overline{u}_j$ where the bar denotes some grid-level filtering operation on a given field $\psi(\mathbf{x})$;

$$\overline{\psi}(\mathbf{x}) = \int G_0(\mathbf{x}, \mathbf{y})\psi(\mathbf{y})d\mathbf{y}.$$

The filtering kernel $G_0(\mathbf{x}, \mathbf{y})$ has a 'filter width' equal to the grid spacing Δ of the LES. To compute C one first introduces a 'test' filtering operation on the large-eddy field that is denoted by the symbol ' ^ ';

$$\widehat{\psi}(\mathbf{x}) = \int G(\mathbf{x}, \mathbf{y})\psi(\mathbf{y})d\mathbf{y},$$

where $G(\mathbf{x}, \mathbf{y})$ is any kernel that serves to damp all spatial fluctuations shorter than some characteristic length $\widehat{\Delta} > \Delta$ and $\mathbf{x}, \mathbf{y}$ are position vectors. The equations for the test-filtered field contain the Reynolds stress term $T_{ij} = \widehat{\overline{u_i u_j}} - \widehat{\overline{u}}_i \widehat{\overline{u}}_j$. Both T_{ij}

and τ_{ij} are unknown in LES; however, the two are related by the identity (Germano 1992)

$$L_{ij} = T_{ij} - \widehat{\tau}_{ij}. \tag{1}$$

Here the Leonard term $L_{ij} = \widehat{\overline{u}_i \overline{u}_j} - \widehat{\overline{u}}_i \widehat{\overline{u}}_j$ is computable from the large-eddy field. Finally, it is assumed that a scaling law is operative and, therefore, the Reynolds stress at the grid and test levels may be written as

$$\tau_{ij} - \frac{1}{3}\tau_{kk}\delta_{ij} = -2C\Delta^2 |\overline{S}|\overline{S}_{ij}. \tag{2}$$

and

$$T_{ij} - \frac{1}{3}T_{kk}\delta_{ij} = -2C\widehat{\Delta}^2 |\widehat{\overline{S}}|\widehat{\overline{S}}_{ij}, \tag{3}$$

respectively. The model coefficient 'C' in (2) and (3) need not be the same. The prescription for determining C described below can be generalized to obtain both coefficients (Moin 1991). In what follows, 'C' is taken to be the same in (2) and (3) for simplicity. On substituting (2) and (3) in (1), an equation for determining C is obtained:

$$L_{ij} - \frac{1}{3}L_{kk}\delta_{ij} = \alpha_{ij}C - \widehat{\beta_{ij}C} \tag{4}$$

where

$$\alpha_{ij} = -2\widehat{\Delta}^2 |\widehat{\overline{S}}|\widehat{\overline{S}}_{ij},$$

$$\beta_{ij} = -2\Delta^2 |\overline{S}|\overline{S}_{ij}.$$

Since C appears inside the filtering operation, equation (4) is a system of five independent integral equations involving only one function C. In previous formulations (Germano *et al.* 1991, Moin *et al.* 1991, Lilly 1992), one simply ignored the fact that C is a function of position and took C out of the filtering operation as if it were a constant. This *ad hoc* procedure cannot even be justified *a posteriori* because the C field computed using this procedure is found to be a rapidly varying function of position (Moin 1991). One of the objectives of this research is to eliminate this mathematical inconsistency.

The C obtained from equation (4) can be either positive or negative. A negative value of C implies a locally negative eddy-viscosity, which in turn implies a flow of energy from the small scales to the resolved scales or back-scatter. It is known from direct numerical simulation (DNS) data (Piomelli *et al.* 1991) that the forward and reverse cascade of energy in a turbulent flow are typically of the same order of magnitude with a slight excess of the former accounting for the overall transfer of energy from large to small scales. The presence of back-scatter, therefore, is a desirable feature of a subgrid-scale model. However, when the C computed from (4) is used in a large-eddy simulation, the computation is found to become unstable. The instability can be traced to the fact that C has a large correlation time. Therefore, once it becomes negative in some region, it remains negative for excessively long periods of time during which the exponential growth of the local

velocity fields, associated with negative eddy-viscosity, causes a divergence of the total energy. Though this issue of stability remained unresolved, a way around the problem was found if the flow possessed at least one homogeneous direction. Previous authors (Germano *et al.* 1991, Moin *et al.* 1991, Cabot and Moin 1991) have used an *ad hoc* averaging prescription to stabilize the model. The disadvantages of this are: (a) It is based on an *ad hoc* procedure. (b) The prescription can only be applied to flows that have at least one homogeneous direction, thus excluding the more challenging flows of engineering interest. (c) The prescription for stabilizing the model makes it unable to represent back-scatter. The present research attempts to eliminate these deficiencies.

2. Accomplishments

In the next section, a variational formulation of the dynamic model is described that removes the inconsistency associated with taking C out of the filtering operation. This model, however, is still unstable due to the negative eddy-viscosity. Next, three models are presented that are mathematically consistent as well as numerically stable. The first two are applicable to homogeneous flows and flows with at least one homogeneous direction, respectively, and are, in fact, a rigorous derivation of the *ad hoc* expressions used by previous authors. The third model in this set can be applied to arbitrary flows, and it is stable because the C it predicts is always positive. Finally, a model involving the subgrid-scale kinetic energy is presented which attempts to model back-scatter. This last model has some desirable theoretical features. However, even though it gives results in LES that are qualitatively correct, it is outperformed by the simpler constrained variational models. It is suggested that one of the constrained variational models should be used for actual LES while theoretical investigation of the kinetic energy approach should be continued in an effort to improve its predictive power and to understand more about back-scatter.

2.1 A variational formulation

Equation (4) may be written as $E_{ij}(\mathbf{x}) = 0$, where

$$E_{ij}(\mathbf{x}) = L_{ij} - \frac{1}{3}L_{kk}\delta_{ij} - \alpha_{ij}C + \widehat{\beta_{ij}C}. \tag{5}$$

The residual $E_{ij}(\mathbf{x})$ at any given point depends on the value of the function C at neighboring points in the field. One cannot, therefore, minimize the sum of the squares of the residuals $E_{ij}E_{ij}$ locally (as in Lilly, 1992) since reducing the value of $E_{ij}E_{ij}$ at one point 'x' changes its values at neighboring points. However, the method of least squares has a natural generalization to the non-local case. The function C that "best satisfies" the system of integral equations (4) is the one that minimizes

$$\mathcal{F}[C] = \int E_{ij}(\mathbf{x})E_{ij}(\mathbf{x})d\mathbf{x}. \tag{6}$$

$\mathcal{F}[C]$ is a functional of C, and the integral extends over the entire domain. To find the Euler-Lagrange equation for this minimization problem, we set the variation of

$\mathcal{F}$ to zero:

$$\delta\mathcal{F} = 2 \int E_{ij}(\mathbf{x})\delta E_{ij}(\mathbf{x})d\mathbf{x} = 0. \tag{7}$$

Using the definition of E_{ij}, we get

$$\int \left(-\alpha_{ij}E_{ij}\delta C + E_{ij}\widehat{\beta_{ij}\delta C}\right) d\mathbf{x} = 0 \tag{8}$$

which may be rearranged as

$$\int \left(-\alpha_{ij}E_{ij} + \beta_{ij} \int E_{ij}(\mathbf{y})G(\mathbf{y},\mathbf{x})d\mathbf{y}\right) \delta C(\mathbf{x})d\mathbf{x} = 0. \tag{9}$$

Thus, the Euler-Lagrange equation is

$$-\alpha_{ij}E_{ij} + \beta_{ij} \int E_{ij}(\mathbf{y})G(\mathbf{y},\mathbf{x})d\mathbf{y} = 0 \tag{10}$$

which may be rewritten in terms of C as

$$f(\mathbf{x}) = C(\mathbf{x}) - \int \mathcal{K}(\mathbf{x},\mathbf{y})C(\mathbf{y})d\mathbf{y} \tag{11}$$

where

$$f(\mathbf{x}) = \frac{1}{\alpha_{kl}(\mathbf{x})\alpha_{kl}(\mathbf{x})} \left[\alpha_{ij}(\mathbf{x})L_{ij}(\mathbf{x}) - \beta_{ij}(\mathbf{x}) \int L_{ij}(\mathbf{y})G(\mathbf{y},\mathbf{x})d\mathbf{y}\right],$$

$$\mathcal{K}(\mathbf{x},\mathbf{y}) = \frac{\mathcal{K}_A(\mathbf{x},\mathbf{y}) + \mathcal{K}_A(\mathbf{y},\mathbf{x}) - \mathcal{K}_S(\mathbf{x},\mathbf{y})}{\alpha_{kl}(\mathbf{x})\alpha_{kl}(\mathbf{x})}$$

and

$$\mathcal{K}_A(\mathbf{x},\mathbf{y}) = \alpha_{ij}(\mathbf{x})\beta_{ij}(\mathbf{y})G(\mathbf{x},\mathbf{y}),$$

$$\mathcal{K}_S(\mathbf{x},\mathbf{y}) = \beta_{ij}(\mathbf{x})\beta_{ij}(\mathbf{y}) \int d\mathbf{z}G(\mathbf{z},\mathbf{x})G(\mathbf{z},\mathbf{y}).$$

Equation (11) is readily recognized as Fredholm's integral equation of the second kind.

2.2. The constrained variational problem

In this section, we address the stability problem created by the negative eddy-viscosity by requiring that in addition to minimizing the functional (6), C satisfy some constraints designed to ensure the stability of the model. The choice of such constraints is clearly not unique. It is shown that the local least squares method (Lilly 1992) coupled with the volume averaging prescription (Germano et al. 1991) can actually be derived as a rigorous consequence of such a constrained variational problem for flows with at least one homogeneous direction. The method is then extended to general inhomogeneous flows.

2.2.1 Homogeneous turbulence

In the case of homogeneous turbulence, it is natural to assume that C can depend only on time. Let us, therefore, impose this as a constraint in the problem of minimizing the functional (6). The functional $\mathcal{F}[C]$ then reduces to the function

$$\mathcal{F}(C) = \langle \mathcal{L}_{ij}\mathcal{L}_{ij}\rangle - 2\langle \mathcal{L}_{ij}m_{ij}\rangle C + \langle m_{ij}m_{ij}\rangle C^2 \tag{12}$$

where $\mathcal{L}_{ij} = L_{ij} - (1/3)L_{kk}\delta_{ij}$ is the traceless part of L_{ij}, $m_{ij} = \alpha_{ij} - \widehat{\beta}_{ij}$ and $\langle \ \rangle$ denotes integral over the volume. The value of C that minimizes the function $\mathcal{F}(C)$ is easily found to be

$$C = \frac{\langle L_{ij}m_{ij}\rangle}{\langle m_{kl}m_{kl}\rangle} \tag{13}$$

where the isotropic part of $\mathcal{L}_{ij}$ has vanished on contracting with the traceless tensor m_{ij}. Equation (13) is precisely the result of Germano *et al.* and Lilly.

2.2.2 Flows with at least one homogeneous direction

As an example, we consider a channel flow with the y-axis along the cross-channel direction and periodic boundary conditions in the x and z directions. Since the flow is homogeneous in the x-z plane, we impose the constraint that C can depend only on time and the y co-ordinate. It is necessary to assume (as did Germano *et al.*) that the filtering kernel $G(\mathbf{x}, \mathbf{y})$ is defined so as to be independent of the cross-channel direction, y. Therefore C may be taken out of the filtering operation and the functional (6) reduces to

$$\mathcal{F}[C] = \int dy \langle (\mathcal{L}_{ij} - m_{ij}C)(\mathcal{L}_{ij} - m_{ij}C)\rangle_{xz} \tag{14}$$

where $\langle \ \rangle_{xz}$ denotes integral over the x-z plane and $i = 1, 2,$ and 3 represents the x, y, and z directions, respectively. The condition for an extremal of the functional (14) may be written as

$$\delta\mathcal{F} = 2 \int dy \delta C(y) \langle m_{ij}m_{ij}C - m_{ij}\mathcal{L}_{ij}\rangle_{xz} = 0 \tag{15}$$

which implies

$$\langle m_{ij}\mathcal{L}_{ij} - m_{ij}m_{ij}C\rangle_{xz} = 0 \tag{16}$$

and since C is independent of x and z and m_{ij} is without trace,

$$C = \frac{\langle m_{ij}L_{ij}\rangle_{xz}}{\langle m_{kl}m_{kl}\rangle_{xz}}. \tag{17}$$

This is the same expression as that of Germano *et al.* and Lilly for flows homogeneous in the x-z plane.

2.2.3 Inhomogeneous flows

In this section, we will adopt the point of view that perhaps the eddy-viscosity describes only a mean flow of energy from large to small scales, and back-scatter needs to be modeled separately as a stochastic forcing (Chasnov 1990, Leith 1990, Mason *et al.* 1992). We shall, therefore, insist on the eddy-viscosity always being positive and for the time being disregard back-scatter. Accordingly, in the problem of minimizing the functional (6), we impose the constraint

$$C \geq 0. \tag{18}$$

It is convenient to write the variational problem in terms of a new variable ξ such that $C = \xi^2$. Then the constraint (18) is equivalent to the condition that ξ be real. In terms of the new variable ξ, equation (9) becomes

$$\int \left(-\alpha_{ij} E_{ij} + \beta_{ij} \int E_{ij}(\mathbf{y}) G(\mathbf{y}, \mathbf{x}) d\mathbf{y} \right) \xi(\mathbf{x}) \delta \xi(\mathbf{x}) d\mathbf{x} = 0, \tag{19}$$

which gives for the Euler-Lagrange equation

$$\left(-\alpha_{ij} E_{ij} + \beta_{ij} \int E_{ij}(\mathbf{y}) G(\mathbf{y}, \mathbf{x}) d\mathbf{y} \right) \xi(\mathbf{x}) = 0. \tag{20}$$

Therefore, at any point $\mathbf{x}$, either $\xi(\mathbf{x}) = 0$ or the first factor in (20) vanishes. That is, at some points of the field $C(\mathbf{x}) = 0$ and at the remaining points

$$C(\mathbf{x}) = \mathcal{G}[C(\mathbf{x})]$$

where

$$\mathcal{G}[C(\mathbf{x})] = f(\mathbf{x}) + \int \mathcal{K}(\mathbf{x}, \mathbf{y}) C(\mathbf{y}) d\mathbf{y}$$

with $f(\mathbf{x})$ and $\mathcal{K}(\mathbf{x}, \mathbf{y})$ as defined in section 2.1. Note, however, we do not know in advance on which part of the domain C vanishes; this information is part of the solution of the variational problem. Therefore, if a C can be found such that

$$C(\mathbf{x}) = \begin{cases} \mathcal{G}[C(\mathbf{x})], & \text{if } \mathcal{G}[C(\mathbf{x})] \geq 0; \\ 0, & \text{otherwise} \end{cases} \tag{21}$$

then it is a nontrivial solution of the Euler-Lagrange equation (20). Equation (21) may be written concisely as

$$C(\mathbf{x}) = \left[f(\mathbf{x}) + \int \mathcal{K}(\mathbf{x}, \mathbf{y}) C(\mathbf{y}) d\mathbf{y} \right]_+ \tag{22}$$

where the operation denoted by the suffix '+' is defined as $x_+ = \frac{1}{2}(x + |x|)$ for any real number x. It is clear that a solution of (22) satisfies the Euler-Lagrange equation (20), but it is not obvious whether this solution is unique (we exclude the trivial solution $C(\mathbf{x}) = 0$). Equation (22) is a nonlinear integral equation, and no rigorous results regarding the existence or uniqueness of its solutions are known to the authors. Nevertheless, we will assume that it has a unique solution in all cases of interest. Numerical experiments so far have given us no reason to question this assumption.

2.3. A model with back-scatter

The instability associated with the negative eddy-viscosity may be understood in the following way. The Smagorinsky eddy-viscosity model does not contain any information on the total amount of energy in the subgrid scales. Therefore, if the coefficient C becomes negative in any part of the domain, the model tends to remove more energy from the subgrid scales than is actually available, and the reverse transfer of energy does not saturate when the store of subgrid-scale energy is depleted. However, in a physical system, if all the energy available in the subgrid scales is removed, the Reynolds stress will go to zero, thus quenching the reverse flow of energy. Clearly, a more elaborate model that keeps track of the subgrid-scale kinetic energy is required. Such a model is described in this section. (The possibility of treating the dynamic model in conjunction with an equation for turbulent kinetic energy was considered by Wong (1992) in a different context.)

From dimensional analysis, the turbulent viscosity is the product of a velocity and a length-scale. We will take the square root of the subgrid-scale kinetic energy for the velocity scale and the grid spacing as the length scale. Thus,

$$\tau_{ij} - \frac{1}{3}\delta_{ij}\tau_{kk} = -2C\Delta k^{1/2}\overline{S}_{ij} \tag{23}$$

and

$$T_{ij} - \frac{1}{3}\delta_{ij}T_{kk} = -2C\widehat{\Delta}K^{1/2}\widehat{\overline{S}}_{ij} \tag{24}$$

where

$$k = \frac{1}{2}(\overline{u_i u_i} - \overline{u}_i\overline{u}_i) = \frac{1}{2}\tau_{ii}, \tag{25}$$

$$K = \frac{1}{2}(\widehat{\overline{u_i u_i}} - \widehat{\overline{u}}_i\widehat{\overline{u}}_i) = \frac{1}{2}T_{ii}. \tag{26}$$

On taking the trace of (1), we have

$$K = \widehat{k} + \frac{1}{2}L_{ii}. \tag{27}$$

Since the average of the square of any quantity is never less than the square of its average, it follows that L_{ii} is non-negative provided the filtering operation involves a non-negative weight $G(\mathbf{x}, \mathbf{y})$. Therefore, K is never less than $\widehat{k}$, a result that might be anticipated since there are more modes below the test level cut-off than below the grid level. Substituting (23) and (24) in (1) and solving the corresponding variational problem, we get (11) with $\alpha_{ij} = -2\widehat{\Delta}K^{1/2}\widehat{\overline{S}}_{ij}$ and $\beta_{ij} = -2\Delta k^{1/2}\overline{S}_{ij}$ to determine $C(\mathbf{x})$.

To complete the model, it remains to give a method for determining k. For this we will use the well known model of the transport equation for k (e.g. Speziale 1991)

$$\partial_t k + \overline{u}_j\partial_j k = -\tau_{ij}\overline{S}_{ij} - C_*\frac{k^{3/2}}{\Delta} + \partial_j(D\Delta k^{1/2}\partial_j k) + Re^{-1}\partial_{jj}k \tag{28}$$

with the grid spacing Δ taken as the length-scale appropriate for the subgrid-scale eddies. Here C_* and D are non-negative dimensionless parameters, and Re is a Reynolds number based on molecular viscosity. The coefficients C_* and D can be determined dynamically. For this purpose, one writes down a model equation for K which is identical in form to (28) with test-level quantities replacing grid-level quantities. One then requires that K and k obtained by solving the corresponding evolution equations be consistent with (27). This gives the following integral equations for determining C_* and D:

$$C_*(\mathbf{x}) = \left[f_*(\mathbf{x}) + \int \mathcal{K}_*(\mathbf{x},\mathbf{y}) C_*(\mathbf{y}) dy \right]_+ \tag{29}$$

and

$$D(\mathbf{x}) = \left[f_D(\mathbf{x}) + \int \mathcal{K}_D(\mathbf{x},\mathbf{y}) D(\mathbf{y}) dy \right]_+ . \tag{30}$$

The derivation and notation are explained in the appendix.

2.3.1 Stability

It will be shown that the model described above is globally stable, that is, the total energy in the large-eddy field remains bounded in the absence of external forces and with boundary conditions consistent with no influx of energy from the boundaries. Using the continuity and momentum equations for the large-eddy fields and the sub-grid kinetic energy equation (28), we derive

$$\frac{d}{dt} \left(\frac{1}{2} \int \overline{u}_i \overline{u}_i dV + \int k dV \right) = - \int \frac{C_*}{\Delta} k^{3/2} dV - Re^{-1} \int (\partial_j \overline{u}_i)(\partial_j \overline{u}_i) dV \tag{31}$$

where the integral is over the region occupied by the fluid. Boundary conditions are assumed to be such that there is no net flux of energy from the boundaries of the domain so that the surface terms vanish. Note that the terms in $\tau_{ij}\overline{S}_{ij}$ which appear as a source term for k and a sink for the resolved scales (if $C > 0$ and vice versa when $C < 0$) have cancelled out in equation (31), and we are left with the result that in the absence of externally imposed forces and nontrivial boundary conditions, the total energy in the large and small scales taken together must monotonically decrease as a result of molecular viscosity. Using the notation

$$E(t) = \frac{1}{2} \int \overline{u}_i \overline{u}_i dV \tag{32}$$

and

$$e(t) = \int k dV, \tag{33}$$

we have by (31), $E(t) + e(t) \leq E(0) + e(0)$ and since $e(t) \geq 0$ (see next section), $E(t) \leq E(0) + e(0)$. Thus, the energy in the large-eddy field cannot diverge even though the eddy-viscosity is allowed to be negative.

2.3.2 Realizability

It is necessary to demonstrate that the k computed using (28) has the following property; $k(\mathbf{x},t) \geq 0$ at all points $\mathbf{x}$ at all times t if $k(\mathbf{x},0) \geq 0$. This condition is required because it is clear from its definition that k cannot be negative, and, indeed, the model cannot be implemented unless the non-negativeness of k can be guaranteed. This condition is part of and included in a more general condition of 'realizability' (Schumann 1977, Lumley 1978) required of subgrid-scale models to be discussed later. It must also be pointed out that L_{ii} is an intrinsically positive quantity only if the filtering kernel $G(\mathbf{x},\mathbf{y}) \geq 0$. The most commonly used filters in physical space such as the 'tophat' filter and the Gaussian filter do meet this requirement while the Fourier cut-off filter does not. Therefore, the Fourier cut-off filter may not be appropriate in this context.

Suppose that initially $(t = 0)$, $k > 0$ at all points. Let $t = t_0$ be the earliest time for which k becomes zero at some point $\mathbf{x} = \mathbf{x}_0$ in the domain. It will be shown that $\partial_t k(\mathbf{x}_0, t_0) > 0$ which ensures that k can never decrease below zero. Integration of equation (28) over an infinitesimal sphere of radius ϵ centered around $\mathbf{x}_0$ gives after dividing by ϵ^3

$$\frac{\partial k}{\partial t} = -\frac{1}{\epsilon^3} \int \bar{u}_n k d\sigma + C \Delta k^{1/2} |\overline{S}|^2 - \frac{C_*}{\Delta} k^{3/2} + \frac{1}{\epsilon^3} \int \nu \frac{\partial k}{\partial n} d\sigma, \qquad (34)$$

where $\nu = Re^{-1} + D\Delta\sqrt{k}$ and $d\sigma$ is an infinitesimal element of area on the surface of the sphere with $\hat{n}$ as the outward normal. Since k first becomes zero at $\mathbf{x} = \mathbf{x}_0$, $\mathbf{x}_0$ is a local minimum. Therefore, $k = \nabla k = 0$ at '$\mathbf{x}_0$', and hence $k \sim \epsilon^2$ and $\nabla k \sim \epsilon$ inside the sphere. Therefore, every term on the right side of (34) is of order ϵ or higher except for the last term which is of order one. Thus, on taking the limit $\epsilon \to 0$ in equation (34), we have

$$\frac{\partial k}{\partial t} = \lim_{\epsilon \to 0} \frac{1}{\epsilon^3} \int \nu \frac{\partial k}{\partial n} d\sigma. \qquad (35)$$

Since k is a minimum at the point $\mathbf{x}_0$, the right-hand side is positive. Therefore, k can never decrease below zero. Note that we have assumed that C remains finite as $k \to 0$. Indeed, (27) implies α_{ij} remains finite as k (and hence β_{ij}) goes to zero. Thus, in this limit, (11) reduces to

$$C(\mathbf{x}) = \frac{\alpha_{ij}(\mathbf{x})L_{ij}(\mathbf{x})}{\alpha_{kl}(\mathbf{x})\alpha_{kl}(\mathbf{x})}$$

which is finite. Also, in this proof we assumed that the second derivatives of k at $\mathbf{x}_0$ are not all zero. The proof, however, can be easily extended to remove this restriction.

The requirement that k be non-negative is contained in a more general set of properties of the tensor τ_{ij}. They are called realizability conditions and may be stated in several equivalent forms (Schumann 1977). Since the Reynolds stress τ_{ij}

is a real symmetric tensor, it can be diagonalized where the diagonal elements τ_α, τ_β and τ_γ are real. The realizability conditions can be stated as

$$\tau_\alpha, \tau_\beta, \tau_\gamma \geq 0. \tag{36}$$

It will be noted that (36) implies

$$k = \frac{1}{2}\tau_{ii} = \frac{1}{2}(\tau_\alpha + \tau_\beta + \tau_\gamma) \geq 0. \tag{37}$$

Positivity of the turbulent kinetic energy is, therefore, a consequence of the more general conditions (36).

The modeled Reynolds stress (23) is diagonal in a co-ordinate system aligned to the principal axes of the rate of strain tensor, and the diagonal elements are

$$\tau_i = -2C\Delta k^{1/2}s_i + \frac{2}{3}k \tag{38}$$

where s_i ($i = \alpha$, β, γ) are eigenvalues of the rate of strain. The realizability conditions (36) are satisfied if

$$-\frac{k^{1/2}}{3\Delta|s_\gamma|} \leq C \leq \frac{k^{1/2}}{3\Delta s_\alpha} \tag{39}$$

at each point of the field. In writing (39), the eigenvalues of the strain rate tensor have been arranged so that $s_\alpha \geq s_\beta \geq s_\gamma$. The incompressibility condition implies $s_\alpha + s_\beta + s_\gamma = 0$ and, therefore, $s_\alpha \geq 0$, $s_\gamma \leq 0$ and s_β may be of either sign. Since C is obtained by solving the integral equation (11), it is difficult (perhaps impossible) to prove any general mathematical result on whether the realizability condition (39) is satisfied. Nevertheless, we offer the following estimates.

A reasonable estimate for k when the turbulence is locally in equilibrium is $k \approx \Delta^2|\overline{S}|^2$. (This gives Smagorinsky's formula on substitution in (23).) With this estimate for k, (39) may be written as $C_{min} \leq C \leq C_{max}$ where

$$C_{min} = -\frac{\sqrt{2}}{3}\frac{\sqrt{s_\alpha^2 + s_\beta^2 + s_\gamma^2}}{|s_\gamma|} \leq -\frac{\sqrt{2}}{3} \tag{40}$$

and

$$C_{max} = \frac{\sqrt{2}}{3}\frac{\sqrt{s_\alpha^2 + s_\beta^2 + s_\gamma^2}}{s_\alpha} \geq \frac{\sqrt{2}}{3}. \tag{41}$$

It is found from numerical experiments on LES of freely decaying homogeneous turbulence (section 2.5) that the distribution of values in the C field at any instant of time is approximately Gaussian with mean about 0.025 and standard deviation about 0.15. The precise values depend on the details of the simulation, but these numbers are representative. For such a field, the number of points falling inside the range $C_{min} \leq C \leq C_{max}$ exceeds 99.9 percent.

2.3.3 Galilean invariance

The Navier-Stokes equations are invariant with respect to the transformations

$$x'_i = x_i - U_i t \tag{42}$$

$$t' = t \tag{43}$$

$$u'_i = u_i - U_i \tag{44}$$

where U_i is independent of space or time. It will be shown that the model described in this section as well as the constrained variational formulation lead to Galilean invariant equations for the large-eddy field.

Substituting (44) in the definition of the Leonard term, we derive $L'_{ij} = L_{ij}$. Since U_i is constant, clearly the rate of strain tensors are invariant. It is shown in the appendix that equation (28) for the subgrid-scale kinetic energy is Galilean invariant. Therefore, $k' = k$, and on using equation (27), $K' = K$. Therefore, each term in the integral equation for C in both the constrained variational formulation and the subgrid-scale kinetic energy formulation are invariant, so that $C' = C$. The invariance of the model now follows on using $\frac{\partial}{\partial x'_i} = \frac{\partial}{\partial x_i}$ and $\frac{D}{Dt'} = \frac{D}{Dt}$.

2.3.4 Behavior near solid walls

Consider a point near the wall with x_1, x_2, and x_3 in the streamwise, wall-normal, and spanwise directions, respectively. Then near the wall, $\overline{u}_1$, $\widehat{\overline{u}}_1$, $\overline{u}_3$, $\widehat{\overline{u}}_3 \sim x_2$, and hence, by the continuity equation, $\overline{u}_2$, $\widehat{\overline{u}}_2 \sim (x_2)^2$. The near wall behavior of the subgrid-scale kinetic energy k involves some subtle issues. From its definition $k = \overline{u_i u_i} - \overline{u}_i \overline{u}_i$, we must have $k \sim (x_2)^2$. In order to obtain such a behavior from (28), one needs to impose the boundary conditions that both k and $\partial k/\partial x_2$ vanish at the walls. However, since equation (28) is only second order in space, we cannot impose both these conditions. Thus, we are forced to choose only $k = 0$ at the wall and this, in general, will give a solution with the asymptotic behavior $k \sim x_2$. One possible remedy is to consider a two equation model (such as a k-ϵ model) in place of equation (28). This gives a system that is fourth order in spatial derivatives and can, therefore, support the additional boundary condition (Durbin 1990. Also see the report by Cabot in this volume). In this report, however, we restrict ourselves to the simpler one equation model (28), and, therefore, the k obtained by solving (28) will in general have the behavior $k \sim x_2$. Nevertheless, we will show that with the model coefficients computed dynamically, the eddy-viscosity is proportional to $(x_2)^3$ and the molecular diffusion of kinetic energy balances the viscous dissipation near the wall independent of whether $k \sim x_2$ or $k \sim (x_2)^2$. To stress this generality, we will write $k \sim (x_2)^{2m}$ where $m = 1/2$ or 1.

The strain rate is dominated by the component $\overline{S}_{12}$ and $\widehat{\overline{S}}_{12}$ which are finite at the wall. The trace of the Leonard term $L_{ii} \sim (x_2)^2$, hence by (27) $K \sim (x_2)^{2m}$. Thus α_{12}, $\beta_{12} \sim (x_2)^m$ are the only surviving terms of α_{ij} and β_{ij} near the wall. With these estimates, $\mathcal{K}(\mathbf{x}, \mathbf{y}) \sim 1$ so that

$$C(\mathbf{x}) \approx f(\mathbf{x}) \approx \frac{L_{12}}{\alpha_{12}} \sim (x_2)^{3-m}.$$

Therefore, the eddy-viscosity $\nu_t = C\Delta\sqrt{k} \sim (x_2)^3$, the well-known "$y$-cubed behavior at the wall".

We now consider the near wall behavior of the kinetic energy equation (28). Using the estimates given in the previous paragraph, $\mathcal{K}_D \sim 1$, so that $D \sim f_D \to 0$ at the wall. On using the expressions for $\mathcal{K}_*$ and f_* given in the appendix, it is again easily verified that near the wall $\mathcal{K}_* \sim 1$, and hence

$$C_* k^{3/2} \sim f_* k^{3/2} \sim |\Delta Re^{-1} \partial_{jj} L_{ii}|$$

which is finite. Hence,

$$\frac{C_* k^{3/2}/\Delta}{|Re^{-1}\partial_{jj}k|} \sim 1 \qquad (45)$$

independent of Δ and Re. Thus, all terms in the kinetic energy equation go to zero at the wall except the viscous dissipation and diffusion terms. These are finite and are of the same order at all Reynolds number and at any grid-resolution. This is the correct near wall behavior of the turbulent kinetic energy equation (Mansour, Kim and Moin 1988).

2.4 Numerical methods

The simplest iteration scheme for solving the integral equation (11) is

$$C_{n+1}(\mathbf{x}) = C_n(\mathbf{x}) + \mu\left[f(\mathbf{x}) + \int \mathcal{K}(\mathbf{x},\mathbf{y})C_n(\mathbf{y})d\mathbf{y} - C_n(\mathbf{x})\right], \qquad (46)$$

where μ is a relaxation factor that is selected to optimize convergence and n is an iteration index. To solve equation (22), the term

$$f(\mathbf{x}) + \int \mathcal{K}(\mathbf{x},\mathbf{y})C_n(\mathbf{y})d\mathbf{y}$$

in (46) needs to be replaced by its positive part. Convergence can be achieved provided $|\mu| \leq \mu_0$ where μ_0 is a number typically of order 0.1 for the present simulation. When the $C(\mathbf{x})$ from the previous time-step was used to start the iteration, convergence at the level of one percent residual error took about twenty iterations. However, if a random velocity field is used in (46), values of μ as small as 10^{-3} are required for stability, which greatly increases the number of iterations required for convergence. It is, therefore, prudent to use a better scheme that converges faster and is less dependent on the nature of the given LES field. Such a scheme can be devised using preconditioning methods.

The integral equation (11) may be written in operator notation as

$$(\mathbf{I} - \mathbf{K})C = f. \qquad (47)$$

On substituting $\mathbf{K} = \mathbf{E} + (\mathbf{K} - \mathbf{E})$ (where $\mathbf{E}$ is for the moment an arbitrary operator) in (47) we obtain

$$C = (\mathbf{I} - \mathbf{E})^{-1}f + (\mathbf{I} - \mathbf{E})^{-1}(\mathbf{K} - \mathbf{E})C. \qquad (48)$$

If C is replaced by C_{n+1} on the left-hand side and C_n on the right-hand side we obtain the iteration scheme

$$C_{n+1} = (\mathbf{I} - \mathbf{E})^{-1}f + (\mathbf{I} - \mathbf{E})^{-1}(\mathbf{K} - \mathbf{E})C_n. \tag{49}$$

Equation (49) reduces to (46) if we choose $\mathbf{E}$ such that

$$\mathbf{E}\psi = \frac{\mu - 1}{\mu}\psi \tag{50}$$

where ψ is an arbitrary function of position. It is well known that the speed of convergence of the scheme (49) depends on the eigenvalue spectrum of the operator

$$\mathbf{B} = (\mathbf{I} - \mathbf{E})^{-1}(\mathbf{K} - \mathbf{E}). \tag{51}$$

The smaller the spectral radius of $\mathbf{B}$, the faster is the convergence. An efficient scheme is therefore obtained by choosing $\mathbf{E}$ such that '$\mathbf{E} \approx \mathbf{K}$', and yet $(\mathbf{I} - \mathbf{E})$ can be readily inverted. One possible choice is

$$\mathbf{E}\psi(\mathbf{x}) = \mu\widehat{\Delta}^3\mathcal{K}(\mathbf{x},\mathbf{x})\psi(\mathbf{x}) \tag{52}$$

where μ is a positive parameter. The motivation for (52) is the following;

$$\mathbf{K}\psi = \int \mathcal{K}(\mathbf{x},\mathbf{y})\psi(\mathbf{y})dy = \mu(\mathbf{x})\widehat{\Delta}^3\mathcal{K}(\mathbf{x},\mathbf{x})\psi(\mathbf{x}) \tag{53}$$

where $\mu(\mathbf{x})$ is expected to be between zero and one (corresponding to the limiting cases where the integrand is a delta function centered on $\mathbf{x}$ and a constant respectively). Equation (53) is exact. Equation (52) is the approximation to $\mathbf{K}$ obtained on ignoring the position dependence of μ. On substituting (52) in (49), we obtain after some algebra

$$C_{n+1}(\mathbf{x}) = \frac{1}{1 - \mu g(\mathbf{x})}\left[f(\mathbf{x}) + \int \mathcal{K}(\mathbf{x},\mathbf{y})C_n(\mathbf{y})dy - \mu g(\mathbf{x})C_n(\mathbf{x})\right] \tag{54}$$

where

$$g(\mathbf{x}) = \frac{\widehat{\Delta}^3}{\alpha_{mn}(\mathbf{x})\alpha_{mn}(\mathbf{x})}\left[2\alpha_{ij}(\mathbf{x})\beta_{ij}(\mathbf{x})G(\mathbf{x},\mathbf{x}) - \beta_{kl}(\mathbf{x})\beta_{kl}(\mathbf{x})\int[G(\mathbf{z},\mathbf{x})]^2 dz\right]. \tag{55}$$

When $G(\mathbf{x},\mathbf{y})$ is a tophat filter (that is, $G(\mathbf{x},\mathbf{y})$ is constant inside the cube of edge $\widehat{\Delta}$ centered at $\mathbf{x}$ and zero outside), (55) reduces to

$$g_{\text{tophat}}(\mathbf{x}) = \frac{2\alpha_{ij}(\mathbf{x})\beta_{ij}(\mathbf{x}) - \beta_{kl}(\mathbf{x})\beta_{kl}(\mathbf{x})}{\alpha_{mn}(\mathbf{x})\alpha_{mn}(\mathbf{x})}. \tag{56}$$

The iteration scheme (54) can be modified to solve (22) on simply replacing

$$f(\mathbf{x}) + \int \mathcal{K}(\mathbf{x},\mathbf{y})C_n(\mathbf{y})dy$$

by its positive part. The preconditioning scheme presented here is analogous to the point Jacobi scheme of inverting a matrix suitably generalized to the continuous case. Numerical tests indicate that (54) is considerably more robust than (46) and converges much faster. If μ is chosen between about 0.2 and 0.5, the scheme is found to be convergent for arbitrary velocity fields including fields of random numbers. With the C from the previous time step used as the initial guess, convergence at the level of 0.01 percent residual error never required more than three iterations for the LES of homogeneous isotropic turbulence described in the next section.

2.5 Results

In this section, results of LES of homogeneous isotropic freely decaying turbulence are presented using the constrained variational approach of section 2.2.3 (henceforth referred to as ieq+) and the kinetic energy approach of section 2.3. The results are compared to the results using the volume averaged (section 2.2.1) approach and to the grid-generated wind tunnel turbulence experiments of Comte-Bellot and Corrsin (1971). The Reynolds number based on the Taylor microscale and rms fluctuating velocity is in the range 40-70 in the experiment. The ratio of the integral to Kolmogorov scale is about 80. Therefore, even if the computational box is to be only three integral scales on a side, a DNS of the experiment will require at least $(512)^3$ grid points.

A pseudo-spectral code due to Rogallo (1981) for homogeneous turbulence is modified and used with a $(32)^3$ grid. The filtering kernel $G(\mathbf{x},\mathbf{y})$ is taken as a Gaussian function of width $\widehat{\Delta} = 2\Delta$, where Δ is the grid spacing. The results of the simulation are expected to be quite insensitive to the exact shape of the filtering kernel or of the ratio $\widehat{\Delta}/\Delta$ (Germano *et al.* 1991). However, the filtering kernel is restricted to be non-negative in the kinetic energy formulation because of considerations of realizability (section 2.3.2).

Figure 1 shows the resolved energy decay as a function of time computed using the volume averaged, ieq+, and kinetic energy versions of the variational method together with the experimental data of Comte-Bellot and Corrsin (1971). All variables are in non-dimensional units. The energy has been scaled with the mean square fluctuation velocity, $\langle u'^2 \rangle$ at the first measuring station. Time is in units of M/U where M is the grid size in the experiment and U is the free stream velocity. To facilitate comparison between computation and experiment, the experimental data has been filtered to remove spatial scales below the resolution of the computational grid. Further, measured data on the energy decay as a function of distance from the grid has been converted into energy decay as a function of time using the measured convective velocity in the flow and Taylor's hypothesis of 'frozen turbulence'. Both the volume averaged and constrained versions give results that are in good agreement with the experimental data. The result obtained using the kinetic
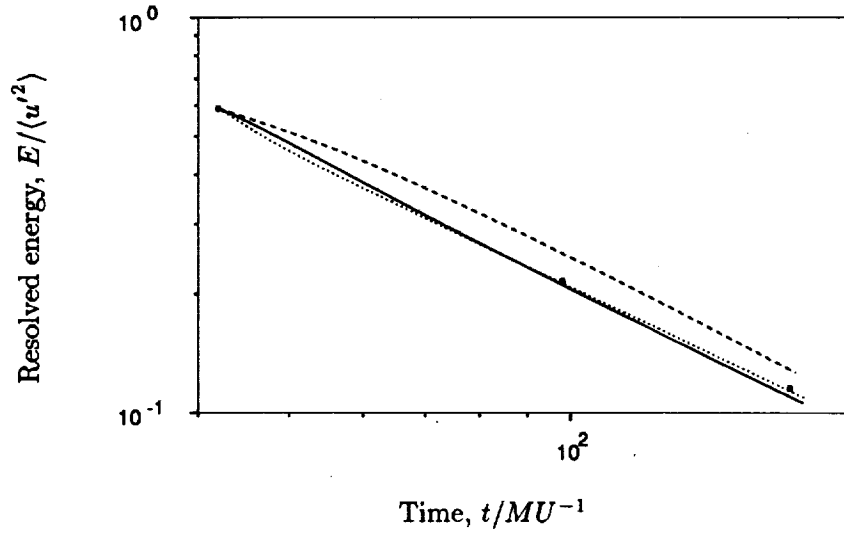
FIGURE 1.   Decay of the resolved energy with time computed using the volume averaged (—), ieq+ ($\cdots$) and kinetic energy (- - -) versions of the variational method.

energy method is seen to be not as good as the other two methods though it has the correct qualitative behavior.

Figure 2 (A), (B), and (C) show the energy spectra at the initial time and two subsequent times computed using the volume averaged, ieq+, and kinetic energy versions of the variational method, respectively, together with the experimental points. Distances have been scaled by $L/2\pi$ where L is length of the computational box which is about ten times the size of the grid generating the turbulence in the experiment. The initial velocity field is chosen to match the initial energy spectrum; therefore, only the last two curves on each figure are of significance.

It is rather surprising that the kinetic energy method which apparently is based on more detailed physical ideas is outperformed by the other two relatively simple models as far as practical LES is concerned. In an effort to understand the reason for this, the subgrid-scale kinetic energy computed using (28) is plotted against the subgrid-scale kinetic energy derived from the experimental data. The result is shown in figure 3. The agreement with the experiment is seen to be remarkably good. Thus, we conclude that the relatively poor performance of the kinetic energy version of the model is not due to errors in prediction of the subgrid-scale kinetic energy. Perhaps the attempt to represent back-scatter by a negative eddy-viscosity is the source of the problem. These issues are still under investigation by the authors.

A typical $C(\mathbf{x})$ field computed using the constrained variational approach is shown in figure 4 over a horizontal cross section of the computational box. The field is seen to be highly variable with C fluctuating by as much as an order of magnitude
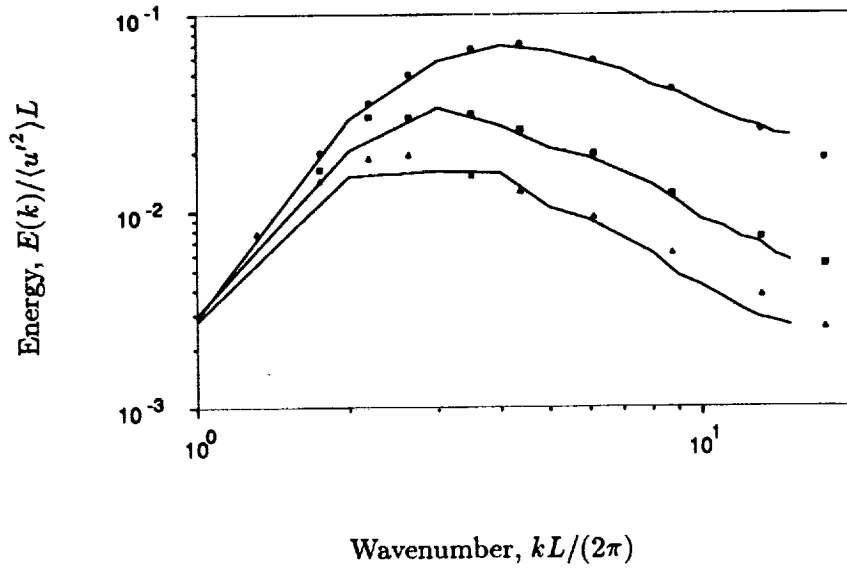
Wavenumber, $kL/(2\pi)$

FIGURE 2(A). Energy spectra at $t\ (MU^{-1}) = 42$ (•), 98 (□), 171 (△) compared with the prediction (—) of the volume averaged model.

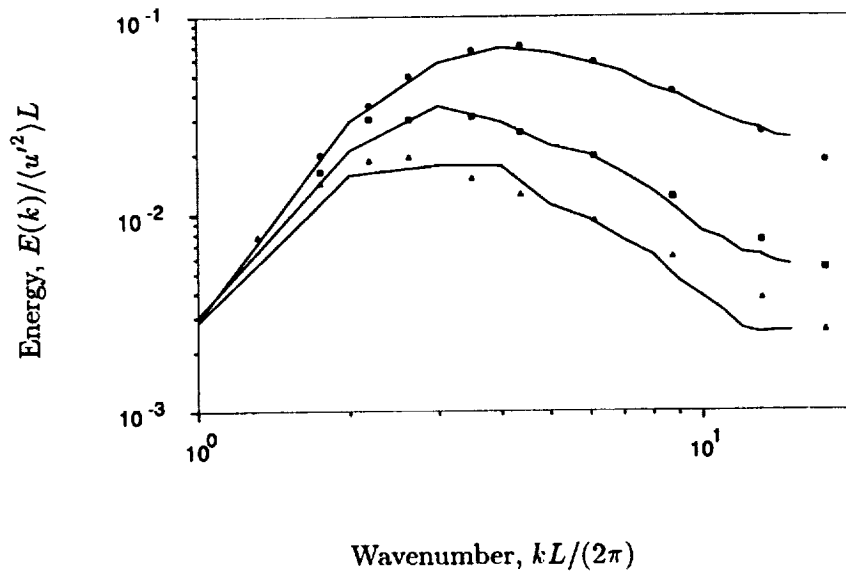Wavenumber, $kL/(2\pi)$
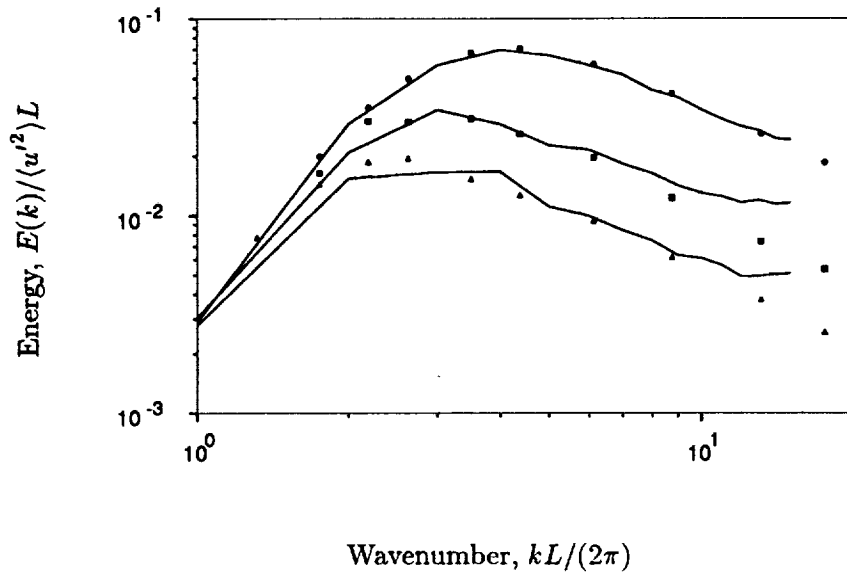
FIGURE 2(B). Same as in 2(A) with the ieq+ model.

FIGURE 2(C).   Same as in 2(A) with the kinetic energy model.
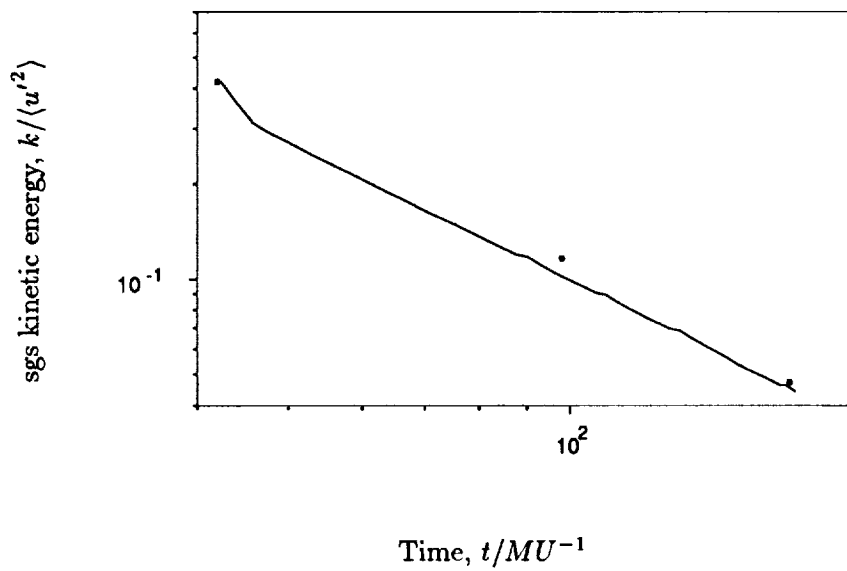

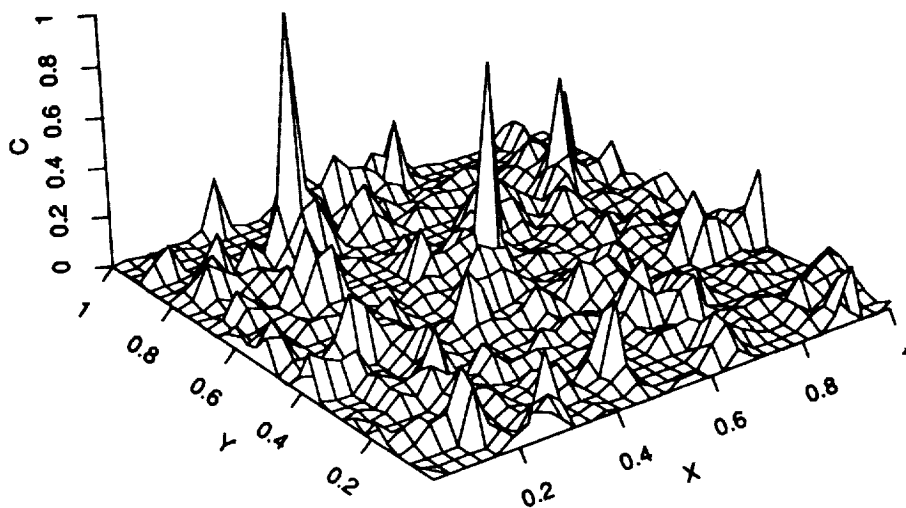FIGURE 3.   Decay of the subgrid-scale kinetic energy with time.

FIGURE 4. The C field over a horizontal cross section of the computational box.

over a few grid spacings. Similar plots of C obtained by solving the (unconstrained) variational problem show a similar qualitative structure.

3. Future plans

The methods for solving the integral equations presented here represent only a first step. A systematic study of the numerical methods available for solving such integral equations must be undertaken. The numerical codes used to conduct the tests presented here have not yet been optimized for performance. This must be done before computations of flows with complex geometry are undertaken. The application of the method in computations with nonuniform grids involve some subtle issues that are being analyzed. It is expected that the methods presented here will be tested in progressively more challenging flows and the outcome of these tests will be used to guide future improvements.

The kinetic energy version of the variational method is applicable to inhomogeneous flows and provides an interesting model of back-scatter. However, the performance of this model in practical LES was not as satisfactory as that of the constrained variational methods. An attempt to understand the reasons for this is likely to produce not only a better model for LES but also a better understanding of back-scatter. Research in this direction is continuing.

In conclusion, it must be stressed that the dynamic localization method is a very general idea and is not restricted in scope to Smagorinsky's model or even to algebraic closure models. Extension of the ideas presented here to improved subgrid-scale models and higher order closures are interesting possibilities.

Appendix. The dynamic determination of C_* and D.

The evolution of subgrid-scale kinetic energy is modeled by the equation

$$\partial_t k + \overline{u}_j \partial_j k = -\tau_{ij}\overline{S}_{ij} - C_* \frac{k^{3/2}}{\Delta} + \partial_j(D\Delta k^{1/2}\partial_j k) + (Re)^{-1}\partial_{jj}k \qquad (A.1)$$

where C_* and D are non-negative parameters. By analogy one can write down the corresponding evolution equation for the subtest-scale kinetic energy

$$\partial_t K + \widehat{\overline{u}}_j \partial_j K = -T_{ij}\widehat{\overline{S}}_{ij} - C_* \frac{K^{3/2}}{\widehat{\Delta}} + \partial_j(D\widehat{\Delta}K^{1/2}\partial_j K) + (Re)^{-1}\partial_{jj}K. \qquad (A.2)$$

Equations $(A.1)$ and $(A.2)$ must be consistent with the relation

$$K = \widehat{k} + \frac{1}{2}L_{ii} \qquad (A.3)$$

(equation (27) in the text). This fact can be exploited to determine C_* and D as shown below.

On substituting equation $(A.3)$ in $(A.2)$ one obtains after some algebraic manipulations

$$\partial_t \widehat{k} + \widehat{\overline{u}}_j \partial_j \widehat{k} = -e + \partial_j f_j + Re^{-1}\partial_{jj}\widehat{k} \qquad (A.4)$$

where

$$e = T_{ij}\widehat{\overline{S}}_{ij} + \frac{C_* K^{3/2}}{\widehat{\Delta}} - \frac{1}{2}Re^{-1}\partial_{jj}L_{ii} + \frac{1}{2}(\partial_t L_{ii} + \widehat{\overline{u}}_j \partial_j L_{ii}) \qquad (A.5)$$

and

$$f_j = D\widehat{\Delta}K^{1/2}\partial_j K. \qquad (A.6)$$

On applying the ' $\widehat{}$ ' operator to both sides of equation $(A.1)$ we obtain

$$\partial_t \widehat{k} + \widehat{\overline{u}}_j \partial_j \widehat{k} = -E + \partial_j F_j + Re^{-1}\partial_{jj}\widehat{k} \qquad (A.7)$$

where

$$E = \widehat{\tau_{ij}\overline{S}_{ij}} + \widehat{(C_* k^{3/2}/\Delta)} \qquad (A.8)$$

and

$$F_j = \widehat{k\overline{u}}_j - \widehat{k}\widehat{\overline{u}}_j + \widehat{D\Delta k^{1/2}\partial_j k}. \qquad (A.9)$$

Equations $(A.4)$ and $(A.7)$ are consistent only if

$$e = E \qquad (A.10)$$

and

$$f_j = F_j \qquad (A.11)$$

It may appear that the term $\frac{1}{2}Re^{-1}\partial_{jj}L_{ii}$ has been arbitrarily lumped with e while it might as well have been converted to a divergence term and made part of f_j. There is, however, no ambiguity as is evident from the following considerations. The coefficient D is a model for pressure diffusion and third order velocity correlation terms which do not depend explicitly on the Reynolds number. On the other hand, C_* models viscous dissipation which contains the Reynolds number explicitly. Thus, any term that contains the Reynolds number must appear in equation $(A.10)$ which determines C_* rather than in equation $(A.11)$ which determines D. A similar objection can be raised for the term $(1/2)\widehat{\bar{u}}_j\partial_j L_{ii}$ in equation $(A.5)$ which could have been written instead as $-(1/2)\widehat{\bar{u}_j L_{ii}}$ on the right hand side of equation $(A.6)$. The choice in this case is dictated by the requirement that both C_* and D must be Galilean invariant in order to be consistent with their physical interpretation. Since it is only the total time derivative $D_t = \partial_t + \widehat{\bar{u}}_j\partial_j$ appearing on the right hand side of equation $(A.5)$ and not ∂_t that is a Galilean invariant operator, the apparent ambiguity is removed. Finally, the purist might argue that the curl of an arbitrary vector can be added on the right hand side of equation $(A.11)$ since we only need to enforce $\partial_j f_j = \partial_j F_j$. This degree of freedom merely refers to the fact that the definition of flux is always ambiguous up to the curl of an arbitrary vector field. Since we assume that the flux is defined identically at both the test and grid levels, the arbitrary solenoidal vector on the right hand side of equation $(A.11)$ must, in fact, be zero.

Equations $(A.10)$ and $(A.11)$ can be rewritten in a more transparent form:

$$\chi = \phi C_* - \widehat{\psi C_*} \qquad (A.12)$$

and

$$Z_j = X_j D - \widehat{Y_j D} \qquad (A.13)$$

with the notation

$$\chi = \widehat{\tau_{ij}\bar{S}_{ij}} - T_{ij}\widehat{\bar{S}}_{ij} - \frac{1}{2}\partial_t L_{ii} - \frac{1}{2}\widehat{\bar{u}}_j\partial_j L_{ii} + \frac{1}{2}Re^{-1}\partial_{jj}L_{ii}$$

$$\phi = \frac{K^{3/2}}{\widehat{\Delta}}$$

$$\psi = \frac{k^{3/2}}{\Delta}$$

$$Z_j = \widehat{k\widehat{\bar{u}}_j} - \widehat{k\bar{u}_j}$$

$$X_j = \widehat{\Delta}K^{1/2}\partial_j K$$

$$Y_j = \Delta k^{1/2}\partial_j k.$$

Clearly χ, ϕ, ψ, Z_j, X_j, and Y_j are known fields at any given time step.

Since equation $(A.12)$ is a single integral equation for C_*, one might be tempted to solve it directly without first going through the variational formulation. However,

since viscous dissipation can only remove energy from the subgrid scales, C_* must be non-negative whereas the C_* obtained by solving $(A.12)$ can have either sign. One must, therefore, try to "best satisfy" $(A.12)$ subject to the constraint $C_* \geq 0$. That is, C_* must be chosen so as to minimize the functional

$$\int (\chi - \phi C_* + \widehat{\psi C_*})^2 dy$$

with the constraint $C_* \geq 0$. Similarly, D is obtained on minimizing

$$\int (Z_j - X_j D + \widehat{Y_j D})(Z_j - X_j D + \widehat{Y_j D}) dy$$

subject to the constraint $D \geq 0$. The solutions to these variational problems can be immediately written down in analogy to the solution (22) in the text if one notices the similarity in structure between equations $(A.12)$, $(A.13)$, and (4) in the text:

$$C_*(\mathbf{x}) = \left[f_*(\mathbf{x}) + \int \mathcal{K}_*(\mathbf{x}, \mathbf{y}) C_*(\mathbf{y}) dy \right]_+ \qquad (A.14)$$

where

$$f_*(\mathbf{x}) = \frac{1}{\phi^2(\mathbf{x})} \left[\phi(\mathbf{x})\chi(\mathbf{x}) - \psi(\mathbf{x}) \int \chi(\mathbf{y}) G(\mathbf{y}, \mathbf{x}) dy \right] ,$$

$$\mathcal{K}_*(\mathbf{x}, \mathbf{y}) = \frac{\mathcal{K}_\mathcal{A}^*(\mathbf{x}, \mathbf{y}) + \mathcal{K}_\mathcal{A}^*(\mathbf{y}, \mathbf{x}) - \mathcal{K}_\mathcal{S}^*(\mathbf{x}, \mathbf{y})}{\phi(\mathbf{x})\phi(\mathbf{x})}$$

and

$$\mathcal{K}_\mathcal{A}^*(\mathbf{x}, \mathbf{y}) = \phi(\mathbf{x})\psi(\mathbf{y}) G(\mathbf{x}, \mathbf{y}),$$

$$\mathcal{K}_\mathcal{S}^*(\mathbf{x}, \mathbf{y}) = \psi(\mathbf{x})\psi(\mathbf{y}) \int dz G(\mathbf{z}, \mathbf{x}) G(\mathbf{z}, \mathbf{y}).$$

$$D(\mathbf{x}) = \left[f_D(\mathbf{x}) + \int \mathcal{K}_D(\mathbf{x}, \mathbf{y}) D(\mathbf{y}) dy \right]_+ \qquad (A.15)$$

where

$$f_D(\mathbf{x}) = \frac{1}{X_j(\mathbf{x}) X_j(\mathbf{x})} \left[X_j(\mathbf{x}) Z_j(\mathbf{x}) - Y_j(\mathbf{x}) \int Z_j(\mathbf{y}) G(\mathbf{y}, \mathbf{x}) dy \right] ,$$

$$\mathcal{K}_D(\mathbf{x}, \mathbf{y}) = \frac{\mathcal{K}_\mathcal{A}^D(\mathbf{x}, \mathbf{y}) + \mathcal{K}_\mathcal{A}^D(\mathbf{y}, \mathbf{x}) - \mathcal{K}_\mathcal{S}^D(\mathbf{x}, \mathbf{y})}{X_j(\mathbf{x}) X_j(\mathbf{x})}$$

and

$$\mathcal{K}_\mathcal{A}^D(\mathbf{x}, \mathbf{y}) = X_j(\mathbf{x}) Y_j(\mathbf{y}) G(\mathbf{x}, \mathbf{y}),$$

$$\mathcal{K}_\mathcal{S}^D(\mathbf{x}, \mathbf{y}) = Y_j(\mathbf{x}) Y_j(\mathbf{y}) \int dz G(\mathbf{z}, \mathbf{x}) G(\mathbf{z}, \mathbf{y}).$$

It is readily verified that χ, ϕ, ψ, Z_j, X_j, and Y_j are all Galilean invariant. Thus C_* and D obtained by solving equations $(A.14)$ and $(A.15)$ are also Galilean invariant which, in turn, implies that the subgrid-scale kinetic energy equation $(A.1)$ itself is Galilean invariant.

REFERENCES

CABOT W., & MOIN P. 1991 Large-eddy simulation of scalar transport with the dynamic subgrid-scale model. *CTR manuscript.* **128**, 1-19.

CHASNOV J. R. 1991 Simulation of the Kolmogorov inertial subrange using an improved subgrid model. *Phys. Fluids A.* **3(1)**, 188-200.

COMTE-BELLOT G. & CORRSIN S. 1971 Simple eulerian time correlation of full and narrow-band velocity signals in grid-generated 'isotropic' turbulence. *J. Fluid Mech.* **48**, 273-337.

DURBIN P. A. 1990 Near wall turbulence closure modeling without 'damping functions'. *Theoret. Comput. Fluid Dynamics.* **3**, 1-13.

GERMANO M. 1992 Turbulence: the filtering approach. *J. Fluid Mech.* **238**, 325-336.

GERMANO M., PIOMELLI U., MOIN P. & CABOT W. 1991 A dynamic subgrid-scale eddy-viscosity model. *Phys. Fluids A.* **3 (7)**, 1760-1765.

LEITH C. E. 1990 Stochastic backscatter in a subgrid-scale model: plane shear mixing layer. *Phys. Fluids A.* **2**, 297-299.

LILLY D. K. 1992 A proposed modification of the Germano subgrid-scale closure method. *Phys. Fluids A.* **4 (3)**, 633-635.

LUMLEY J. L. 1978 Computational modeling of turbulent flows. *AIAM.* **18**, 123-176.

MANSOUR N. N., KIM J. & MOIN P. 1988 Reynolds-stress and dissipation-rate budgets in a turbulent channel flow. *J. Fluid Mech.* **194**, 15-44.

MASON P. J. & THOMSON D. J. 1992 Stochastic backscatter in large-eddy simulations of boundary layers. *J. Fluid Mech.* **242**, 51-78.

MOIN P. 1991 A new approach for large eddy simulation of turbulence and scalar transport. *Proc. Monte Verita coll. on turbulence. Birkhauser, Bale.*

MOIN P., SQUIRES K., CABOT W. & LEE S. 1991 A dynamic subgrid-scale model for compressible turbulence and scalar transport. *Phys. Fluids A.* **3 (11)**, 2746-2757.

PIOMELLI U., CABOT W. H., MOIN P. & LEE S. 1991 Subgrid-scale back-scatter in turbulent & transitional flows. *Phys. Fluids A.* **3(7)**, 1766-1771.

ROGALLO R. S. 1981 Numerical experiments in homogeneous turbulence. *NASA Tech. Mem.* **81315.**

SCHUMANN U. 1977 Realizability of Reynolds-stress turbulence models. *Phys. Fluids A.* **20(5)**, 721-725.

SMAGORINSKY J. 1963 General circulation experiments with the primitive equations. I. The basic experiment. *Mon. Weather Rev.* **91**, 99-165.

SPEZIALE C. G. 1991 Analytic methods for the development of reynolds-stress closures in turbulence. *Ann. Rev. Fluid Mech.* **23**, 107-157.

WONG V. C. 1992 A proposed statistical-dynamic closure method for the linear or nonlinear subgrid-scale stresses. *Phys. Fluids A.* **4(5)**, 1080-1082.